

1 **Climate Change Impact on Water Resources of Tank Cascade Systems in the**  
2 **Godavari sub-basin, India**

3 Koppuravuri Ramabrahmam<sup>1</sup>, Venkata Reddy Keesara<sup>1</sup>, Raghavan Srinivasan<sup>2</sup>, Deva Pratap<sup>1</sup>,  
4 Venkataramana Sridhar<sup>3\*</sup>

5 <sup>1</sup>Department of Civil Engineering, National Institute of Technology Warangal, Telangana,  
6 506004, India

7 <sup>2</sup> AgriLife Research, Texas A&M University, College Station, TX, 77843, USA

8 <sup>3</sup> Department of Biological Systems Engineering, Virginia Polytechnic Institute and State  
9 University, Blacksburg, VA, 24061, USA (\* Corresponding author: vsri@vt.edu)

10  
11 **Abstract**

12 The availability of water at the regional and river basin scales in the future will be significantly  
13 impacted by climate change. Effective water management in the sub-basin is essential for ensuring  
14 long-term sustainability in the face of changing climatic conditions. The Maner River basin is a  
15 significant contributor to the Godavari River, and agriculture serves as the primary source of  
16 income for the majority of individuals residing in the subbasin. Nearly 50-65% of irrigational fields  
17 in the Maner basin are cultivated using local Tank Cascade Systems (TCS) and reservoirs that are  
18 managed by monsoon precipitation. The regional level climate change impact on the water  
19 resources of these tank cascade systems is important for sustainable management of water  
20 resources. In this study, The NEX-GDDP RCM models of CCSM4, MPI-ESM-LR and MIROC-  
21 ESM-CHEM were utilized to examine climate patterns during historical and future periods under

22 RCP 4.5 and RCP 8.5 scenarios. The Maner sub-basin and KTCS (Katakshapur Tank Cascade  
23 System) were modeled using the SWAT hydrological model to simulate runoff and water  
24 availability. The average monsoon (July-October) streamflow increase in the Maner basin during  
25 the near, mid, and far futures is projected to be 47%, 66%, and 114% under the RCP 4.5 scenario,  
26 and 53%, 72%, and 69% under the RCP 8.5 scenario, respectively. Excess flow may overflow  
27 from Ramchandrapur, Mallampalli, and Dharmaraopalli tanks to the downstream Katakshapur  
28 tank since it can accommodate the up to 18.91 Mm<sup>3</sup>. To enhance water management in response  
29 to climate change, one potential adaptation strategy is to utilize the surplus inflow to refill  
30 downstream artificial ponds, which can aid in the replenishment of groundwater and the provision  
31 of water supply to tail end tanks.

32 **Keywords:** Tank Cascade System, Water management; Climate change; NEX-GDDP; SWAT.

33

## 34 **1. Introduction**

35 The change in the global climate will have a substantial influence on the hydrological patterns at  
36 the local and regional levels (Sridhar et al., 2018; Dibike, 2005). According to the climate  
37 projection, there will be more precipitation over the Indian peninsula and coastal regions, while no  
38 increase or decrease is anticipated in the inland areas (Kumar et al., 2013). India is projected to  
39 experience an average temperature increase of 1.5 °C by the year 2050, based on ensemble means  
40 (IPCC 2021). The monsoon precipitation dominates the Indian climate, though it erratic and highly  
41 seasonal in nature, any changes in climate variability are likely to have a significant impact on  
42 water availability within the basin (Maurya et al., 2023). Climate change is likely to have a  
43 significant impact on the availability of streamflow in basin (Sharannya et al., 2018) and water  
44 availability in the tank (Alehu and Bitana 2023). Tanks and a series of tanks connected by a single  
45 watercourse as Tank Cascade Systems (TCS) were built in ancient times to store rainfall and  
46 surface runoff in order to alleviate the local region's water scarcity (VonOppen and Subba Rao,  
47 1987). In India's southern state of the Telangana is enriched of TCS (mostly falling in the Krishna  
48 River Basin (KRB) and Godavari River basin (GRB)) in the basin has a substantial influence on  
49 surface energy, hydrological water balance, and regional climate (Thiery 2015; Ramabrahmam et  
50 al., 2021). The direct climate impact on tank hydrology also influenced by basin hydrology (Alejo  
51 and Alejandro, 2022), therefore, it is important to consider climate change impact on both river  
52 basins and tank systems.

53 The key literature on the effects of climate change on basins and tanks around the world and in  
54 India was discussed below. In Dau et al.'s (2020) found that the hydrology of the Huong River  
55 Basin in Vietnam is expected to withstand the most severe climate projections, ensuring sufficient  
56 water supply for agricultural and domestic purposes in the future. Nandi and Manne 2020

57 investigated on Sina basin, India, and found that, the water balance components would be  
58 adversely affected by climate change in the near future. The projected hydrological changes caused  
59 by climate change are an important input in defining water resource policies (Hengade et al., 2018).  
60 Climate change projections using HadCM3 resulted an increase in future runoff of more than 36%  
61 in the upper Godavari basin (Saraf et al., 2018). In the Wardha watershed of the GRB, the future  
62 streamflow is reduced, and the intra- and interannual streamflow variability is less variable than  
63 the observed streamflow (Sowjanya et al., 2018). The spatial pattern in the Wainganga River basin  
64 of GRB remained unchanged despite an increase in rainfall, evapotranspiration, and runoff (Das  
65 and Umamahesh, 2018; Hengade et al., 2018). Similarly, In the latter half of the 21st century, there  
66 will be an upward trend in precipitation in the Warangal basins, specifically during the months of  
67 July and August (Chanapathi et al., 2020).

68 The hydrology of the watershed will change as a result of climate change's impact (Dessie et al.,  
69 2015; Alejo and Alejandro 2022,). The climate impact of the Great African Lakes revealed that  
70 the largest lake cools during the day (Thiery et al., 2015). The future inflow into the Mediterranean  
71 basin's Beysehir lake is reduced, and land-use scenarios had no significant impact on hydrology  
72 (Bucak et al., 2017), some important global studies are (Hassan et al., 2022; Alehu and Bitana  
73 2023) on lakes and (He et al., 2019) on cascade reservoir. The impacts of climate change on Phakal  
74 Lake located in KRB, India, analysed with SWAT model results to a decrease of up to 57% in tank  
75 inflows in the future (Jayanthi and Keesara, 2021). Therefore, the water harvesting structures can  
76 absorb the rainfall variability and improve the of agricultural productivity under future climate  
77 projections (Vema et al. 2022).

78 Tank systems are crucial water management and storage systems in semi-arid regions, and changes  
79 in the basin's hydrology and climate can have an impact on their water balance. Therefore, it is

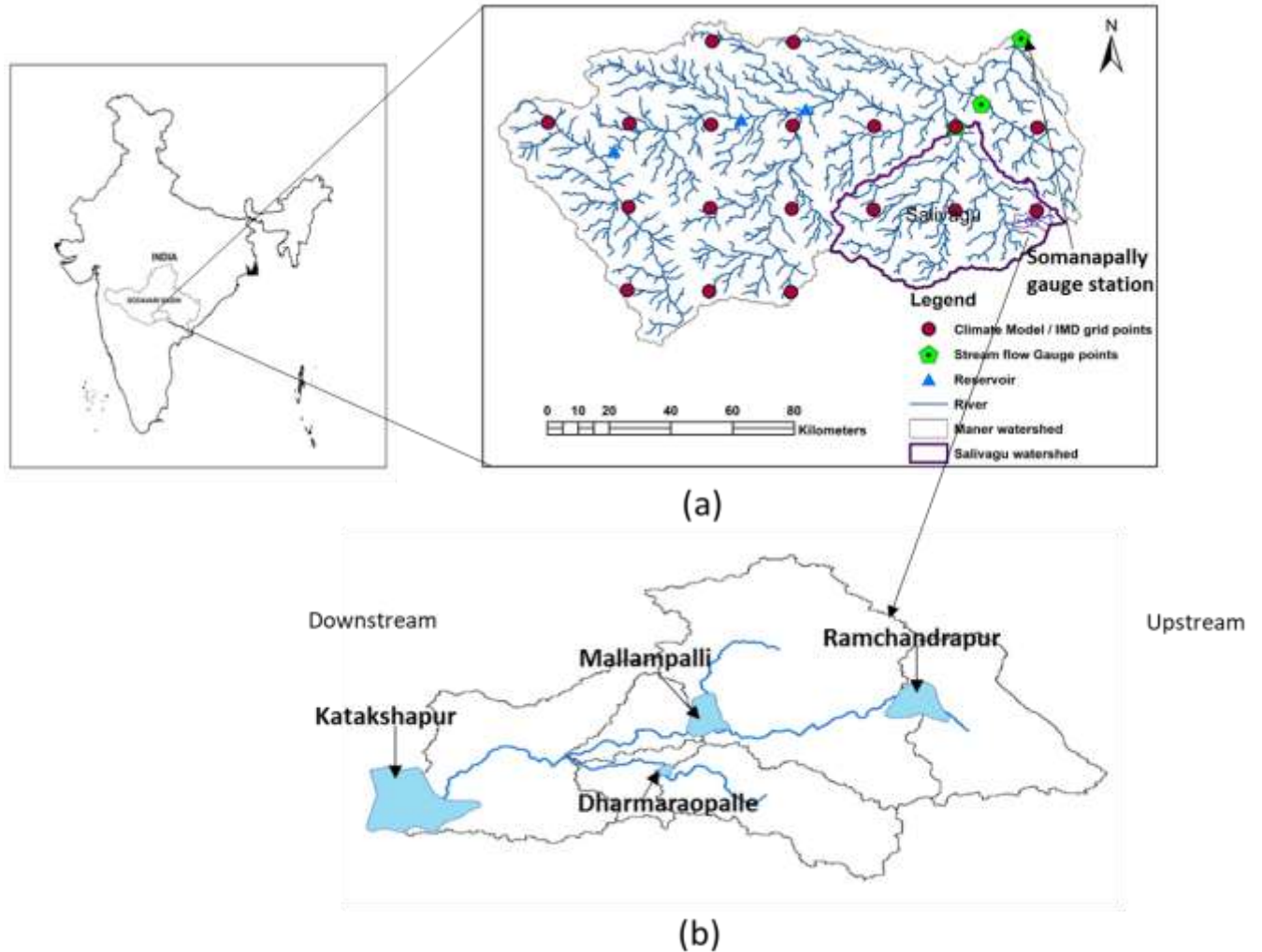
80 critical in this case to analyse how climate change affects the management of cascade tank  
81 irrigation. However, majority of climate change research has focused on projected precipitation  
82 and streamflow variations in basins rather than tank systems. To date, the climate impact analysis  
83 on reservoirs and large tanks at the regional scale has been addressed, but the climate impact on  
84 medium irrigation TCS and the relationship with the basin have not been addressed. In light of  
85 climate variability, it is essential to conduct a comprehensive investigation to formulate enduring  
86 water management strategies that support agricultural production sustainability. As per the  
87 literature, the Godavari River basin and Maner watershed needs the climate change impact analysis  
88 and some adaptation strategies to tanks and TCS. The SWAT model was used in the majority of  
89 the studies for basin-scale analyses, with only a few studies using it for climate change effect  
90 analysis on reservoirs and lakes. The novel aspect of our study was to perform interlinked modeling  
91 and analysis using rescaled climate projections, the SWAT model, and storage infrastructure in the  
92 Maner River in peninsular India as the importance of place-based assessment, particularly for the  
93 Godavari river basin was urgently needed. Hence, the future projected streamflow in the Maner  
94 basin, inflows to TCS using SWAT model and development of adaptable strategies for sustainable  
95 water management policies at the local scale were the focus of this study. The following sections  
96 provide detailed information about the study area, methodology, results, and discussions.

97

98 **2. Study area**

99 The Maner watershed is the sub-basin of the Godavari basin, India (Fig 1 (a)). The basin is located  
100 between latitudes 17°41'20N to 18°40'N and longitudes 78°13'E to 79°59'40E. The Maner river is  
101 a right-bank tributary of the Godavari River covering an area of 13,106 Square Kilometers. The  
102 entire Maner catchment area is located in the state of Telangana. Maner river has Upper Maner,  
103 Middle Maner and Lower Maner dams are the main water resource projects for providing drinking  
104 and irrigation water to the Karimnagar district as well as water to the Ramagundam NTPC plant.  
105 The average annual rainfall of the catchment is 932mm (1951-2005) and the southwest monsoon  
106 (JJASO) is the only primary rainy season. The Pedda bodaru Vagu (stream), a 13kilometer long  
107 stream, is a tributary of the Salivagu River, flowing from the topmost Ramchandrapur tank to the  
108 lowest Katakshapur tank in the KTCS (Fig 1 (b)). The Maner river is fed by the Salivagu river,  
109 which has numerous small to medium-sized tanks and TCS within its watershed, most of which  
110 are ungauged.

111



112

113 **Fig.1** Study area of (a) Maner river basin and (b) KTCS (Katakshapur Tank Cascade System).

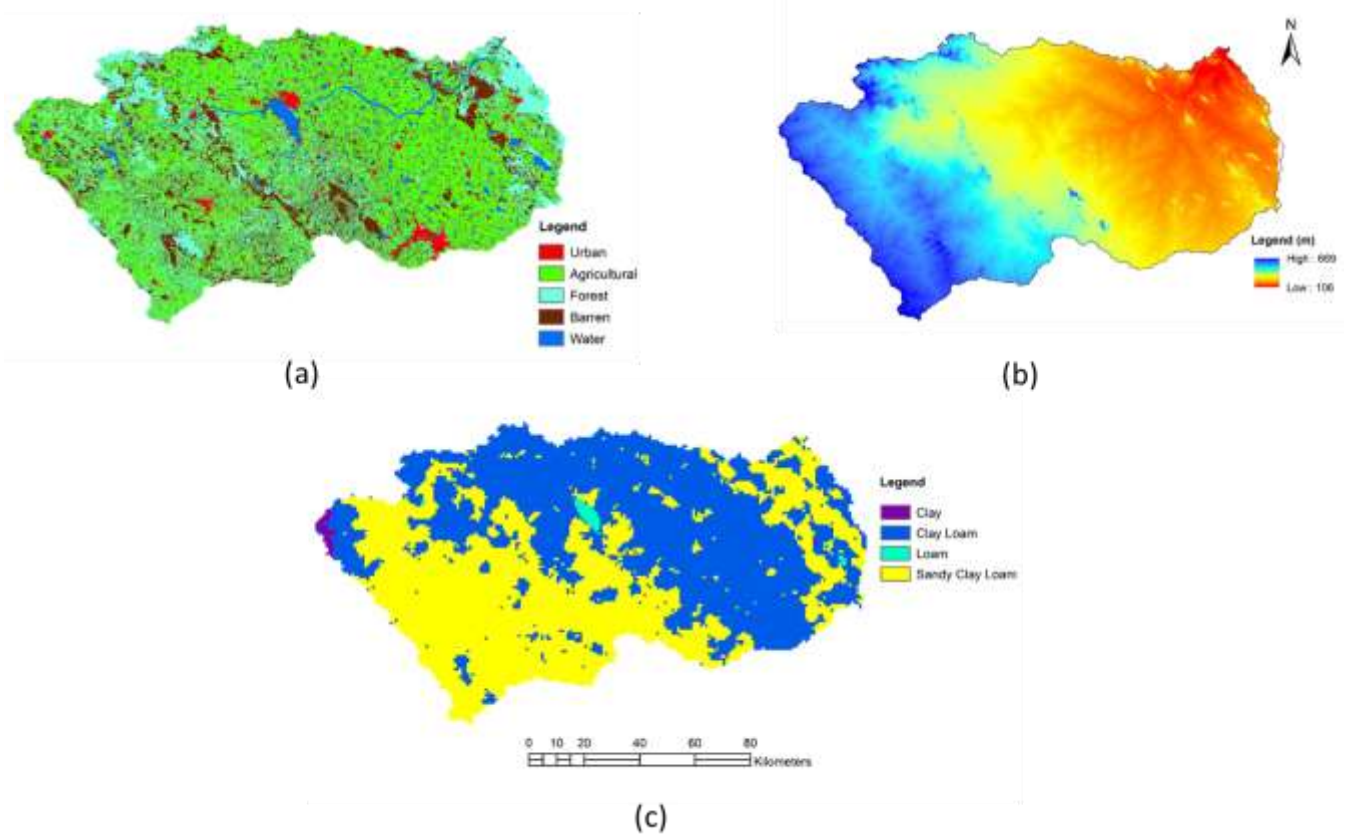
114 **3. Data and methodology**

115 **3.1. Data**

116 The digital elevation model (DEM) data obtained through the Shuttle Radar Topography Mission  
 117 (SRTM) has a spatial resolution of 30 meters. The basin has medium topographic relief, with  
 118 elevations ranging from 106m to 669m (Fig 2 b). It has been utilized for the automated demarcation  
 119 of the watershed limits and stream network.

120 The Land Use-Land Cover (LULC) maps for the base period and subsequent periods were  
121 provided by the National Remote Sensing Center (NRSC). Based on these maps, the Maner sub-  
122 basin was found to contain 65% and 67% of agricultural (AGRL) land, 17% and 14% of barren  
123 area (BARR), 7% of water (WATR) and forest land (FRST), and 4% and 5% of urban area  
124 (URBN) in 2005-06 and 2017-18, respectively. (Fig 2 a).

125 The study utilized the soil map from the ISRIC (International Soil Reference and Information  
126 Centre) world soil data, which had a resolution of 1km (Fig 2c). The predominant soils in the  
127 Maner basin are clay loam and sand clay loam. Paddy is the crop that is most frequently grown  
128 during the Kharif season due to improvements in surface and groundwater usage in the area, which  
129 is composed of a mixture of red and black soil. Depending on water availability and crop cycle,  
130 cotton, chili, and maize are also grown in the basin.



131

132 **Fig. 2** (a) Land use-land cover map (2017-18), (b) Digital elevation model and c) soil map of the  
133 Maner watershed.

134 According to data collected from India WRIS (IWRID, 2022), the Maner river experiences  
135 seasonal flow, with 80% of the total streamflow occurring between July and October and the peak  
136 flow is observed in August. Gridded data with a spatial resolution of  $0.25^{\circ} \times 0.25^{\circ}$  from the Indian  
137 Meteorological Department (IMD) Pune (IMD 2021, Pai et al., 2014; Srivastava et al., 2005),  
138 covering the period of 1980 to 2020, was utilized to analyze the daily precipitation, maximum, and  
139 minimum temperatures.

140 The NASA Earth Exchange Global Daily Downscaled Projections (NEX-GDDP) are simulations  
141 that have been downscaled statistically. They are based on runs of General Circulation Models  
142 (GCM) conducted as part of the Coupled Model Intercomparison Project Phase 5 (CMIP-5). These  
143 simulations cover two of the four greenhouse gas emissions scenarios known as Representative  
144 Concentration Pathways (RCPs), specifically RCP 4.5 and 8.5 (Taylor et al., 2012). These datasets,  
145 with a spatial resolution of  $0.25^{\circ} \times 0.25^{\circ}$  are available at the Indian Institute of Tropical  
146 Meteorology (IITM), Pune. The climate models including MIROC-ESM-CHEM, CCSM4, and  
147 MPI-ESM-LR were used in this study and details are provided in Table 1. These datasets were  
148 used to hydrological processes under RCP 4.5 and 8.5 scenarios for historic (1980–2005) and  
149 future (2006–2099) climatic conditions.

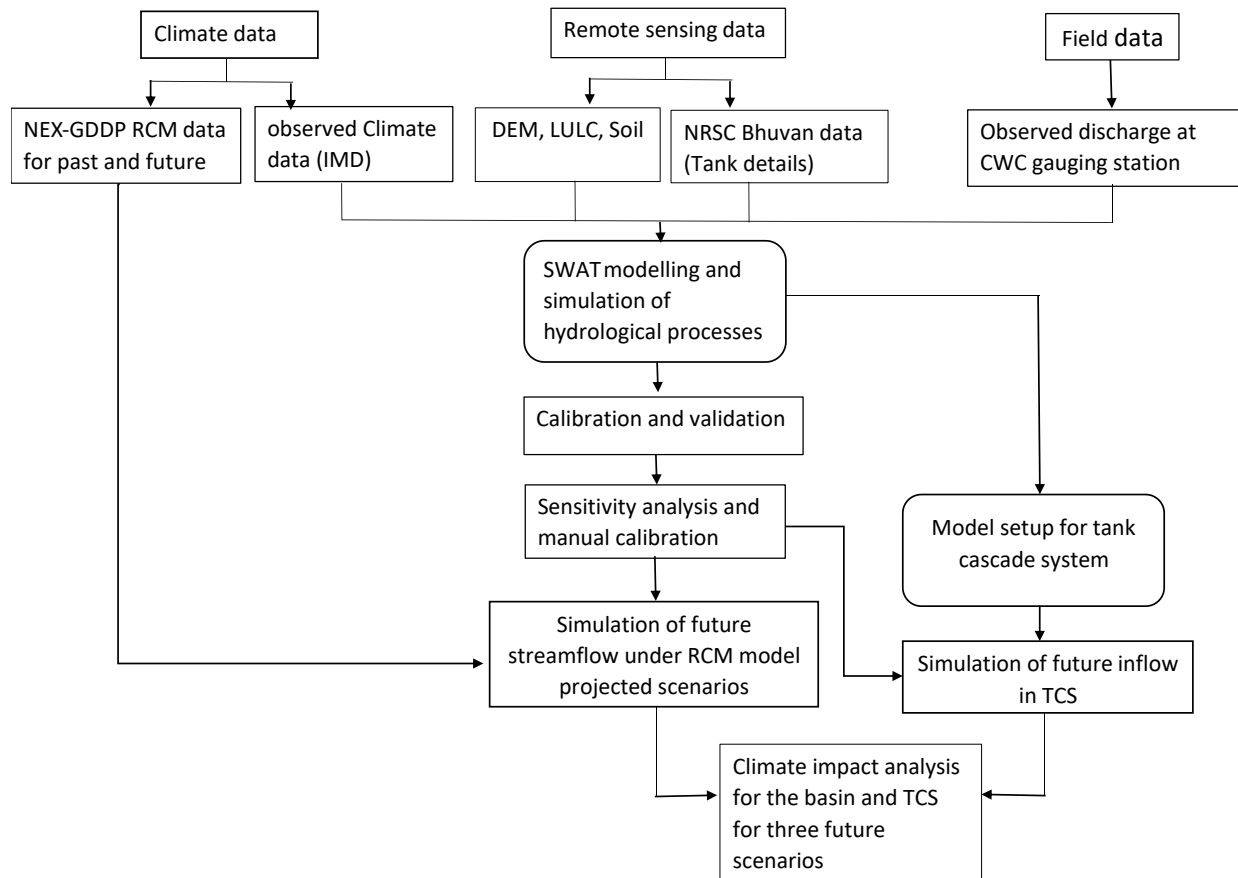
150 **Table.1** The details of RCM models used in the study

| <b>RCM-Name</b> | <b>Institute name</b>   |
|-----------------|---|
| MIROC-ESM-CHEM  | Atmosphere and Ocean Research Institute<br>(University of Tokyo) and others (Japan) |
| CCSM4           | National Center for Atmospheric Research (NCAR), USA                                |

151

## 152 **3.2 Methodology**

153 Initially, the SWAT hydrological simulation was performed in the Maner river basin using IMD  
154 gridded precipitation (1980-2020), LULC, and soil data. The simulated streamflow was calibrated  
155 (1980-2010) and validated (2011-2020) in SWAT-CUP using observed discharge at the  
156 Somanapalli gauge station to evaluate the model performance. Secondly, the best SWAT  
157 parameters were used to perform the future climate change impact in the Maner basin and  
158 Katakshapur Tank Cascade System (KTCS) using an ensemble of CCSM4, MPI-ESM-LR and  
159 MIROC-ESM-CHEM RCM model data under RCP 4.5 and 8.5 future projected scenarios. As a  
160 result, the tank inflow volumes are estimated for the future period from 2022 to 2099. The details  
161 methodology followed in this study is given in Fig 3.



162

163

**Fig. 3** The methodology used in the present study

164

### 165 3.2.1 RCM model selection

166 The NEX-GDDP climate models were sorted based on the correlation of mean monthly IMD  
 167 precipitation during 1951-2005. MIROC-ESM, MIROC-ESM-CHEM, CCSM4, INM-CM4,  
 168 BNU-ESM and MPI-ESM-LR RCM models were selected from among all 21 climate models with  
 169 coefficient of correlations of 0.7 and determination 0.5 or higher were chosen. The other statistics  
 170 of MAE is 25.64% to 38.2% and RMSE is 26% to 35% were selected for the basin average annual  
 171 precipitation. The chosen models aligned with studies on the effects of climate change on the

172 Godavari River basin and reservoirs (Jayanti and Keesara, 2021 Dubey et al., 2018) using GCMs  
173 (Sharmila et al., 2015; Hengade et al., 2018) and RCMs (Das and Umamahesh, 2018).

### 174 **3.2.2 Hydrological modelling**

175 The physically-based SWAT model is a spatially distributed continuous-time simulation model  
176 designed to simulate the quantity and quality of surface and subsurface water on a daily basis. Its  
177 purpose is to forecast the environmental impacts of climate change and land use and management  
178 practices (Srinivasan et al., 1998; Neitsch et al., 2011). The watershed is subdivided into subbasins,  
179 which are then divided further into Hydrological Response Units (HRUs). Using the water balance  
180 equation (Neitsch et al., 2005), the model computes surface and subsurface flow by simulating  
181 hydrological processes.

$$182 \quad SW_t = SW_0 + \sum_{i=1}^t (R_{\text{day}} - Q_{\text{sur}} - E_a - W_{\text{seep}} - Q_{\text{gw}}) \quad (1)$$

183 where  $SW_t$  is the soil water content at time 't',  $SW_0$  is initial soil water content,  $R_{\text{day}}$  is  
184 precipitation on day (i),  $Q_{\text{sur}}$  is the surface runoff on day (i),  $E_a$  is the evapotranspiration on day  
185 (i),  $W_{\text{seep}}$  is the amount of the water seep to the vadose zone from soil profile on day (i),  $Q_{\text{gw}}$  is the  
186 amount of return flow on day (i).  $R_{\text{day}}$ ,  $E_a$ ,  $W_{\text{seep}}$  are the vertical flow and  $Q_{\text{gw}}$ ,  $Q_{\text{sur}}$  are the  
187 horizontal flow water budget components respectively. The Penman-Monteith method is used to  
188 estimate the  $E_a$  fluxes based on potential evapotranspiration. Seepage from the soil surface is  
189 regulated by infiltration and is dependent on the permeability of the soil layer.

190

### 191 **3.2.3 Evaluation of model Performance**

192 The streamflow simulated by SWAT is calibrated (1980-2010) and validated (2011-2020) by  
 193 comparing it with observed discharge at Somanapalli gauge station, using the Sequential  
 194 Uncertainty Fitting (SUFI-2) algorithm of SWAT-CUP (SWAT Calibration and Uncertainty  
 195 Program). The Nash-Sutcliffe (NS) index, expressed in equation 2, is employed as the primary  
 196 objective function for the model's calibration and validation, as it determines the residual variance  
 197 between the simulated and observed data. Additionally, the coefficient of determination (R<sup>2</sup>),  
 198 calculated using equation 3, is used to determine the correlation between the simulated and  
 199 observed streamflow. Finally, the average tendency of the simulated flow compared to the field  
 200 data is evaluated using P-BIAS (Gupta et al. 1999), which employs equation 4.

$$201 \quad NS = 1 - \frac{\sum_{i=1}^n (Q_m - Q_s)^2}{\sum_{i=1}^n (Q_{m,i} - \bar{Q}_m)^2} \quad (2)$$

$$202 \quad R^2 = \frac{\sum_{i=1}^n [(Q_{m,i} - \bar{Q}_m)(Q_{s,i} - \bar{Q}_s)]^2}{\sum_{i=1}^n (Q_{m,i} - \bar{Q}_m)^2 \sum_{i=1}^n (Q_{s,i} - \bar{Q}_s)^2} \quad (3)$$

$$203 \quad$$

$$204 \quad PBIAS = 100 \times \frac{\sum_{i=1}^n (Q_m - Q_s)_i}{\sum_{i=1}^n Q_{m,i}} \quad (4)$$

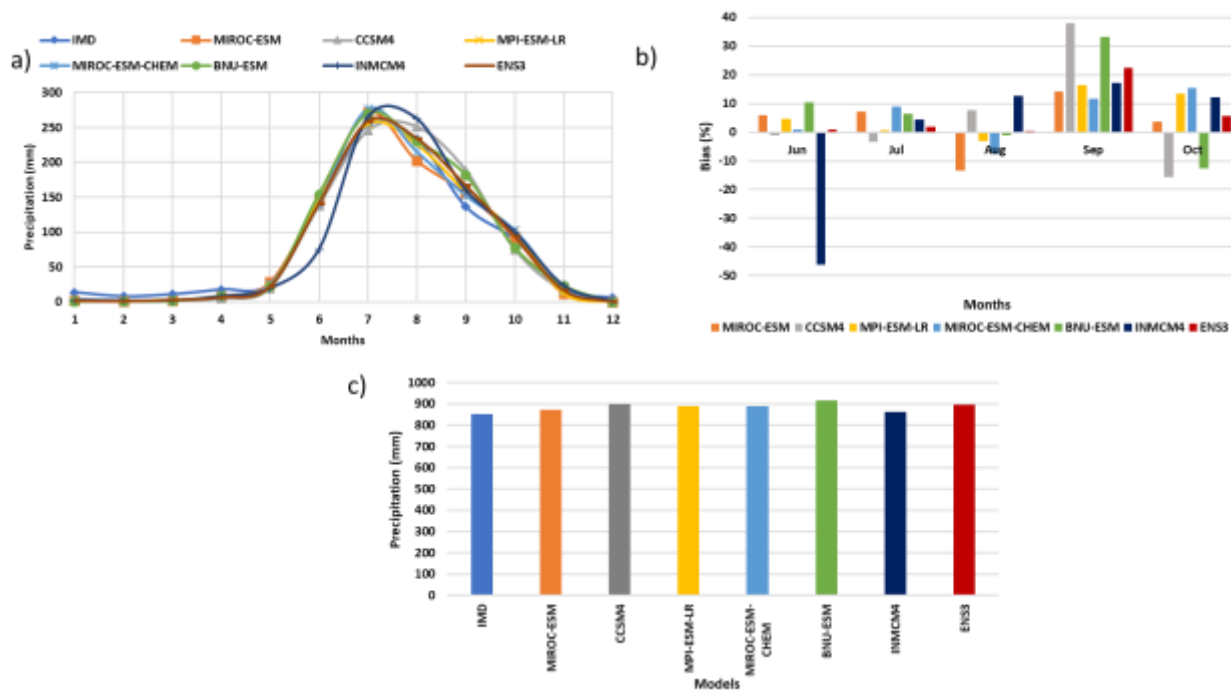
205 where,  $Q_m$  is observed discharge,  $\bar{Q}_m$  is mean of observed discharge,  $Q_s$  is simulated discharge,  
 206  $\bar{Q}_s$  = mean of simulated discharge,  $i$  is the  $i$ th measured and simulated variable,  $n$  is the total  
 207 number of observations.

## 208 **4. Results and Discussion**

### 209 **4.1. Precipitation and Temperature analysis for historic and future periods**

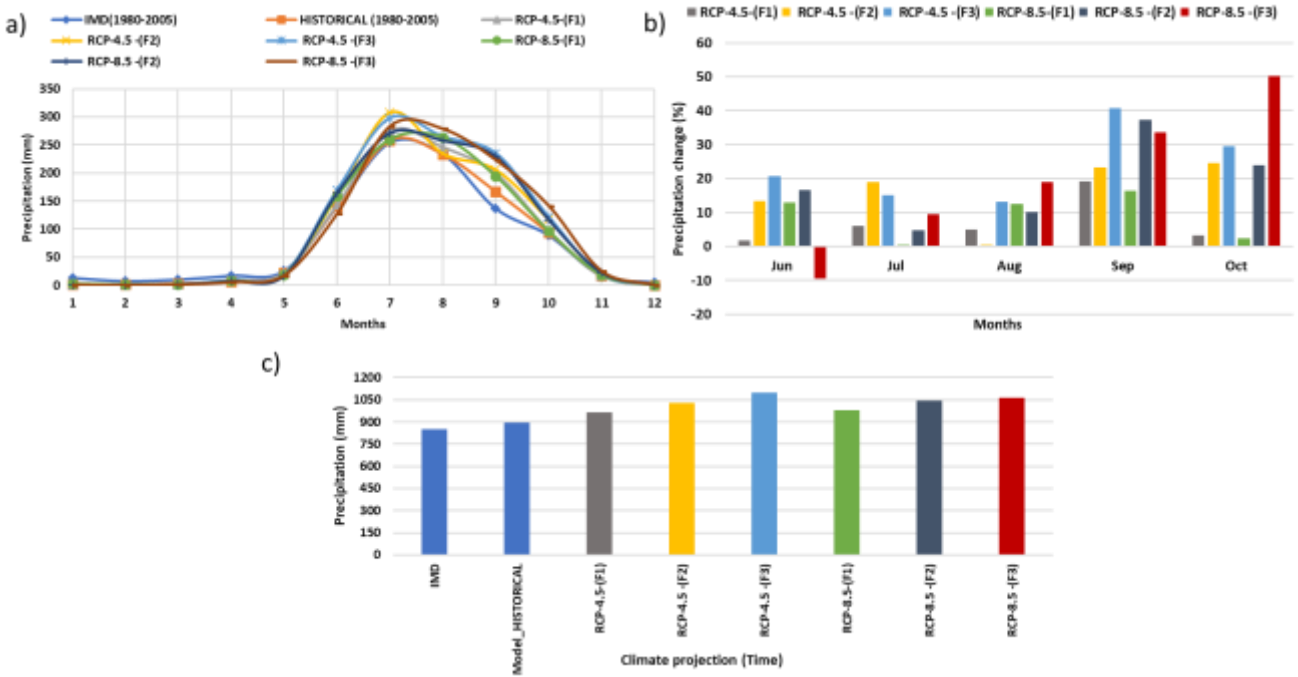
210 Among six selected models, the CCSM4, MPI-ESM-LR, and MIROC-ESM-CHEM models  
 211 precipitation have a moderate bias of -15 to + 38 percent in monsoon months (JJASO) during the

212 base period (Fig 4b). For better results, these three models ensemble (ENS3) mean used for  
 213 historical and future climate impact analyses. The ensemble modeled (ENS3) precipitation has a  
 214 lower percentage bias, ranging from 0.96 to 22.3. The mean monsoon precipitation is 895.09 mm,  
 215 which is similar to the observed precipitation (852.4 mm), with a bias of +5% due to higher  
 216 precipitation in September.



217  
 218 **Fig. 4** a) Observed and RCM models average mean monthly precipitation and b) percentage bias  
 219 c) Average monsoon precipitation in the Maner basin during base period of 1980 to 2005.

220 All future scenarios (Fig 5a) show an increase in mean monthly precipitation for ENS3 when  
 221 compared to the historical base period. The ENS3 mean monthly future predicted precipitation  
 222 increases by up to 20% in the near future, 40% in the mid-future, and 51% in far future under RCP  
 223 4.5 and 8.5 scenarios (Fig 5b). The maximum percentage increase is 40 % and 51% in far future  
 224 months of September and October under the RCP4.5 and RCP 8.5 scenarios, respectively (Fig 5b).  
 225 Monsoon (JJASO) precipitation in near, mid, and far future periods is 964.19, 1029.75, and  
 226 1097.45mm under RCP 4.5, and 979.71, 1042.97, and 1064.23mm under RCP 8.5 (Fig 5c).



228

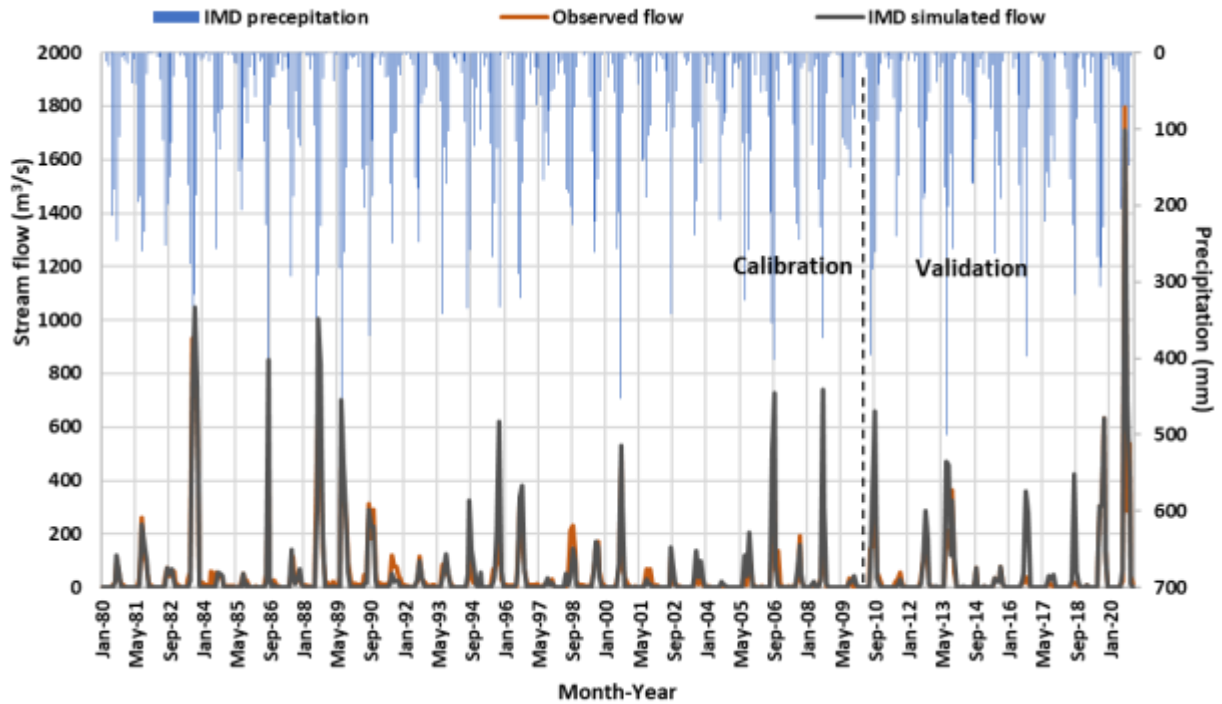
229 **Fig. 5** a) Ensembled model (ENS3) mean monthly precipitation, b) percentage change and c)   
 230 Average monsoon precipitation in the Maner basin for future projected RCP 4.5 and 8.5 scenarios   
 231 (F1=2006-2039, F2=2040-2069, F3=2070-2099).

232 The average annual minimum temperature is 22.37 °C, 23.12 °C, 23.61°C and 22.63°C, 24.01°C,   
 233 25.95°C during near, mid, far futures under RCP 4.5 and 8.5 scenarios, respectively. The average   
 234 annual maximum temperature is 32.99°C, 34.87°C, 36.22°C and 34.01°C, 34.9°C, 35.34 °C during   
 235 near, mid, far futures under RCP 4.5 and 8.5 scenarios, respectively. The increase in maximum   
 236 and minimum temperature is 3.23 °C and 1.88 °C under RCP 4.5 scenario, 1.33 °C and 3.32 °C   
 237 under RCP 8.5 scenario, respectively.

238 **4.2 Calibration and validation of SWAT model**

239 Using the SWAT model, we simulated the streamflow in the Maner basin and identified the   
 240 sensitive parameters and their best fitted values, as presented in Table 2. The observed discharge

241 of the CWC gauge station at Somanapally was used to calibrate the mean monthly streamflow  
 242 from 1980 to 2010 and validate it from 2011 to 2020 with the SUFI-2 algorithm in SWAT-CUP,  
 243 as shown in Figure 6. The model performance statistics for NS and R2 were 0.8 and 0.84 during  
 244 calibration, and 0.87 and 0.87 during validation, respectively, as presented in Table 3.



245  
 246 **Fig. 6** The SWAT simulated streamflow in the Maner basin at Somanapalli gauge station during  
 247 1980-2020 period.

248 **Table.2** The list of SWAT model calibrated parameters

| S.no | Parameter Name | Minimum values | Maximum values | Fitted Value |
|------|----------------|----------------|----------------|--------------|
| 1    | R_CN2.mgt      | -0.08          | 0.020          | -0.043       |
| 2    | V_ALPHA_BF.gw  | 0.47           | 0.833          | 0.730        |
| 3    | A_GW_DELAY.gw  | -30            | 10             | -29.24       |
| 4    | A_GWQMN.gw     | -729           | -48            | -361.941     |
| 5    | V_GW_REVAP.gw  | 0.13           | 0.2            | 0.193        |

|    |                   |        |       |          |
|----|-------------------|--------|-------|----------|
| 6  | V_ESCO.hru        | 0.32   | 0.53  | 0.390    |
| 7  | R_SOL_AWC(..).sol | -0.05  | 0.016 | 0.001    |
| 8  | A_RCHRG_DP.gw     | -0.035 | 0.022 | 0.001    |
| 9  | A_REVAPMN.gw      | -517   | -250  | -367.213 |
| 10 | V_CH_N2.rte       | 0.026  | 0.06  | 0.027    |
| 11 | V_CH_K2.rte       | 15     | 25    | 18.21    |
| 12 | V_CH_K1.sub       | 23     | 32    | 30.335   |
| 13 | V_CH_N1.sub       | 0.008  | 0.09  | 0.020    |
| 14 | V_LAT_TTIME.hru   | 15     | 41    | 35.566   |
| 15 | V_ALPHA_BF_D.gw   | 0      | 1     | 0.535    |

249 R-Relative, V- Replace, A-Absolute methods to change existing value

250 **Table.3** The SWAT-CUP statistical results of SWAT simulated flow of the Maner basin during  
251 1980-2020.

| Process                 | P-factor | R-factor | R <sup>2</sup> | NS   | P-Bias |
|-------------------------|----------|----------|----------------|------|--------|
| Calibration (1980-2010) | 0.51     | 0.89     | 0.84           | 0.8  | 9.1    |
| Validation (2011-2020)  | 0.49     | 0.54     | 0.87           | 0.87 | -14.1  |

252

253 The p-factor and r-factor model uncertainty parameters were found to be 0.51 and 0.89,  
254 respectively, during calibration, and 0.49 and 0.54, respectively, during validation. The  
255 performance statistics indicate that the SWAT model has been reasonably well-calibrated and  
256 validated for the Maner basin. During high flows, the simulated flow is greater than the observed  
257 flow and underestimated during baseflows. The model P-Bias was underpredicted during  
258 calibration due to streamflow being captured by the upper Maner dam and overpredicted during  
259 validation due to the presence of mid-Maner dams as balancing reservoirs on the Maner river.  
260 Most of peak flows are observed in August and September, with an average peak flow of 547 m<sup>3</sup>/s

261 observed between 1980 and 2020. The first wet year was recorded in 1983, with a flow of 1048  
262 m<sup>3</sup>/s, and they occurred every three years until 1990. The streamflow was reduced due to the  
263 construction of the lower Maner dam in 1985, and the first dry year was noticed in 2014. The mid-  
264 Maner dam was built in 2017 and acted as a balancing reservoir, there after the flooding condition  
265 was observed in 2020. As per above results and actual condition, it is apparent that the three big  
266 dams (Upper, Middle and Lower Maner) have complete control over the Maner River.

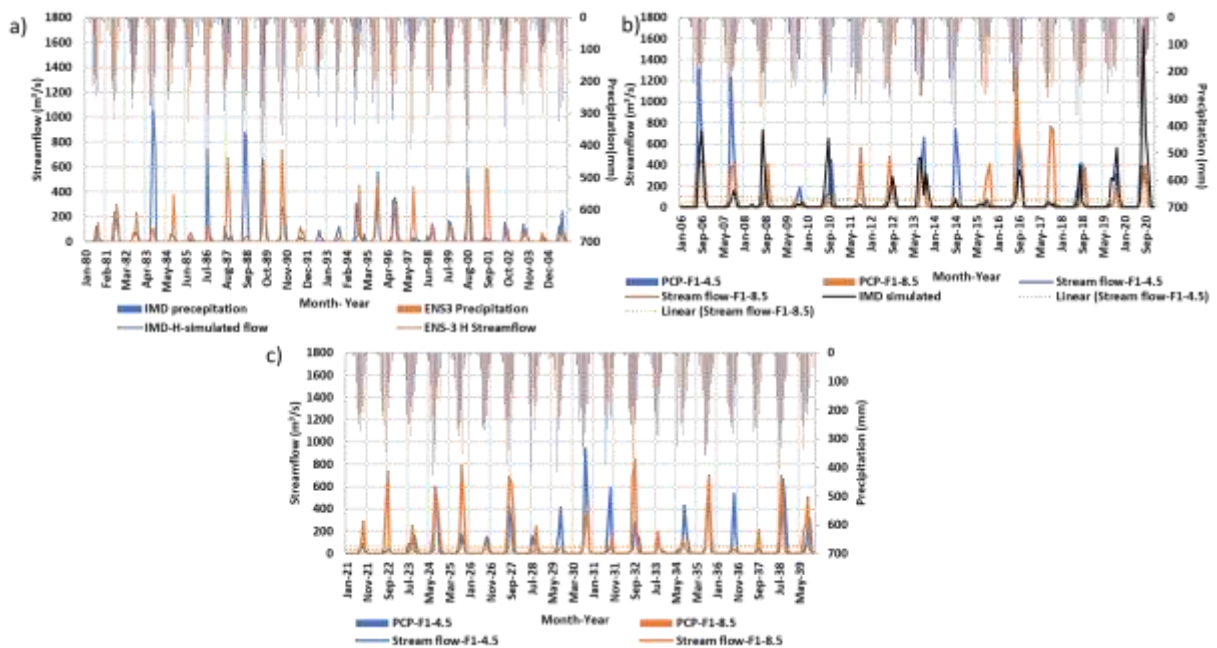
267 During the base period (1980-2005), Fig 7a shows that the ENS3 model reasonably simulated  
268 streamflow, which was consistent with the amount of precipitation. The average peak flow during  
269 this period was 406 m<sup>3</sup>/s, but there were ten occasions when the peak flow exceeded this value.  
270 The ensemble model predicted that in 1989 and 2005, there would be high and low peak flows of  
271 734 m<sup>3</sup>/s and 235.4 m<sup>3</sup>/s respectively.

### 272 **4.3. Climate change impact on future streamflow**

273 The impact of climate change on streamflow is studied over three time periods i.e., 2006-2039  
274 (F1) near future, 2040-2069 (F2) mid future, and 2070-2099 (F3) far future. The near future (2006-  
275 2039) is divided into two parts one is historic (2006-2020) and the current near future (2021-2039)  
276 for the purpose of understanding climate models predictions. In the historical period, the  
277 streamflow trend with the simulated IMD showed a decrease in the RCP 8.5 scenario and an  
278 increase in the RCP 4.5 scenario (Fig 7b). The historical low and medium streamflow magnitudes  
279 under the RCP 4.5 scenario match the IMD simulated flows, with the exception of a few peak  
280 flows.

281 The Peak flows are typically observed in August, September, and October. According to RCP4.5  
282 scenario, the average peak flow is 605.9 m<sup>3</sup>/s, while the maximum and minimum peak flows in

283 August 2006 and 2013 were 1310 m<sup>3</sup>/s and 331.6 m<sup>3</sup>/s, respectively. The average peak flow under  
 284 RCP8.5 scenarios is 523.74 m<sup>3</sup>/s, the maximum and minimum peak flows were 1332 m<sup>3</sup>/s and 335  
 285 m<sup>3</sup>/s in August 2016 and 2013, respectively. The average simulated peak flow by IMD is 516.85  
 286 m<sup>3</sup>/s, with the maximum and minimum flows occurring in August 2020 and September 2019,  
 287 respectively, with values of 1711 m<sup>3</sup>/s and 257.30 m<sup>3</sup>/s. Both scenarios peak flows do not match  
 288 the IMD simulated flow, but the RCP 4.5 scenario flows are close to the IMD's average peak flow.  
 289 In the current near future period (2021-2039), the streamflow has shown an increasing trend in the  
 290 RCP 4.5 scenario, but a declining trend in the RCP 8.5 scenario (Fig 7 c), which is the opposite of  
 291 the historical period. The average peak flow in RCP4.5 scenarios is 503 m<sup>3</sup>/s, and six events  
 292 exceeded the average peak flows during this time period, with maximum and minimum peak flows  
 293 of 943 m<sup>3</sup>/s and 315.5 m<sup>3</sup>/s, respectively. The average peak flow under RCP8.5 scenarios is 564.3  
 294 m<sup>3</sup>/s, with seven events exceeding the average peak flow, 847.8 m<sup>3</sup>/s and 341.6 m<sup>3</sup>/s being the  
 295 maximum and minimum peak flows, respectively.



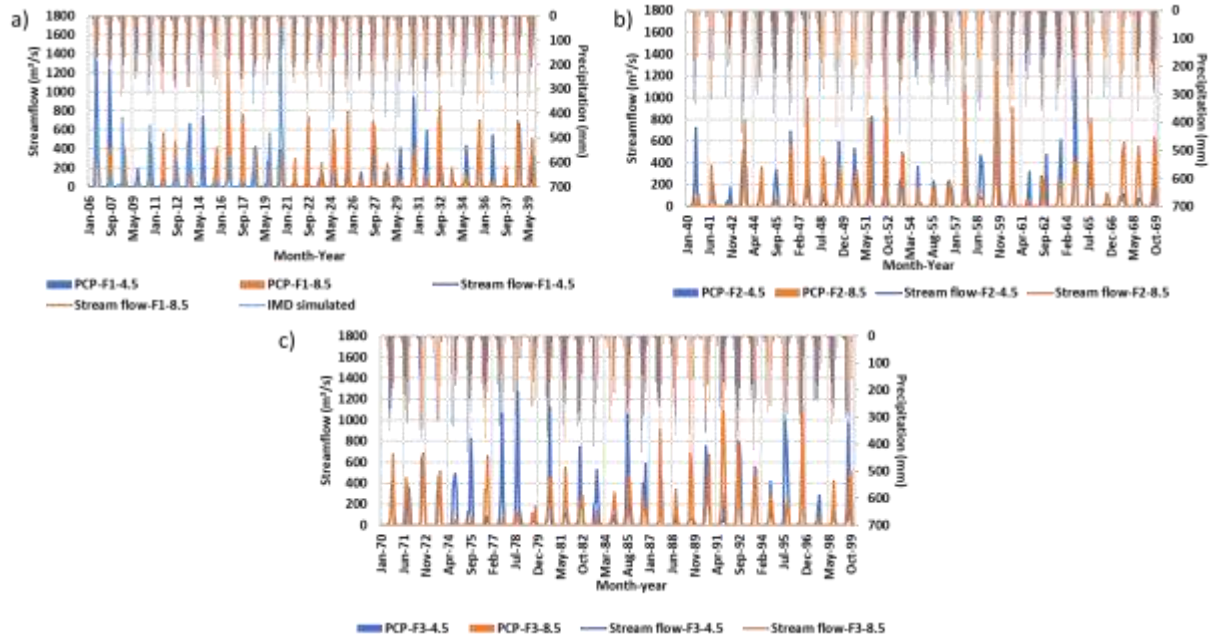
296

297 **Fig. 7** The ensemble model (ENS-3) precipitation and SWAT Simulated streamflow a) during base  
298 period (1980-2005), b) during historic (2006-2020) and c) current near future (2021-2039) of the  
299 Maner river basin

300 The streamflow of near future period (2006-2039) under RCP 4.5 and 8.5 scenarios has shown a  
301 decreasing trend, which is different with historic and near future periods. The average peak flow  
302 under RCP 4.5 is 579.45 m<sup>3</sup>/s, with eleven events exceeding this magnitude; the maximum and  
303 minimum peak flows in this duration are 1310 m<sup>3</sup>/s and 377 m<sup>3</sup>/s, respectively (Fig 8 a). Under  
304 RCP8.5 scenario, the average peak flow is 544 m<sup>3</sup>/s, with fourteen events exceeding the average  
305 peak flows; the maximum and minimum peak flow are 1332 m<sup>3</sup>/s and 334 m<sup>3</sup>/s, respectively. The  
306 ensemble model predicted that average streamflow peaks would be higher in the near future than  
307 in the baseline period.

308 The average peak flows in the mid-future (2040-2069) are 550.92 m<sup>3</sup>/s and 720.28 m<sup>3</sup>/s,  
309 respectively, and eleven and twelve events are exceeded under RCP 4.5 and 8.5 scenarios (Fig 8  
310 b). Under RCP 4.5 and 8.5 scenarios, the maximum and minimum peak flows are 1175, 1237 and  
311 335, 453.6 m<sup>3</sup>/s, respectively. The mid-future simulated streamflow's under the RCP 8.5 projected  
312 scenario had higher peak flows than the RCP 4.5 scenarios.

313 Under RCP 4.5 and 8.5 scenarios, average peak flows of 726.68 m<sup>3</sup>/s and 586.14 m<sup>3</sup>/s, and ten and  
314 eleven events are exceeded the flow respectively in the far future (2070-2099) (Fig 8 c). Under  
315 RCP 4.5 and 8.5 scenarios, the maximum and minimum peak flows are 1271, 1125, and 442, 357.1  
316 m<sup>3</sup>/s respectively. The far future simulated streamflow's under the RCP 4.5 projected scenario had  
317 higher peak flows than the RCP 8.5 scenarios.



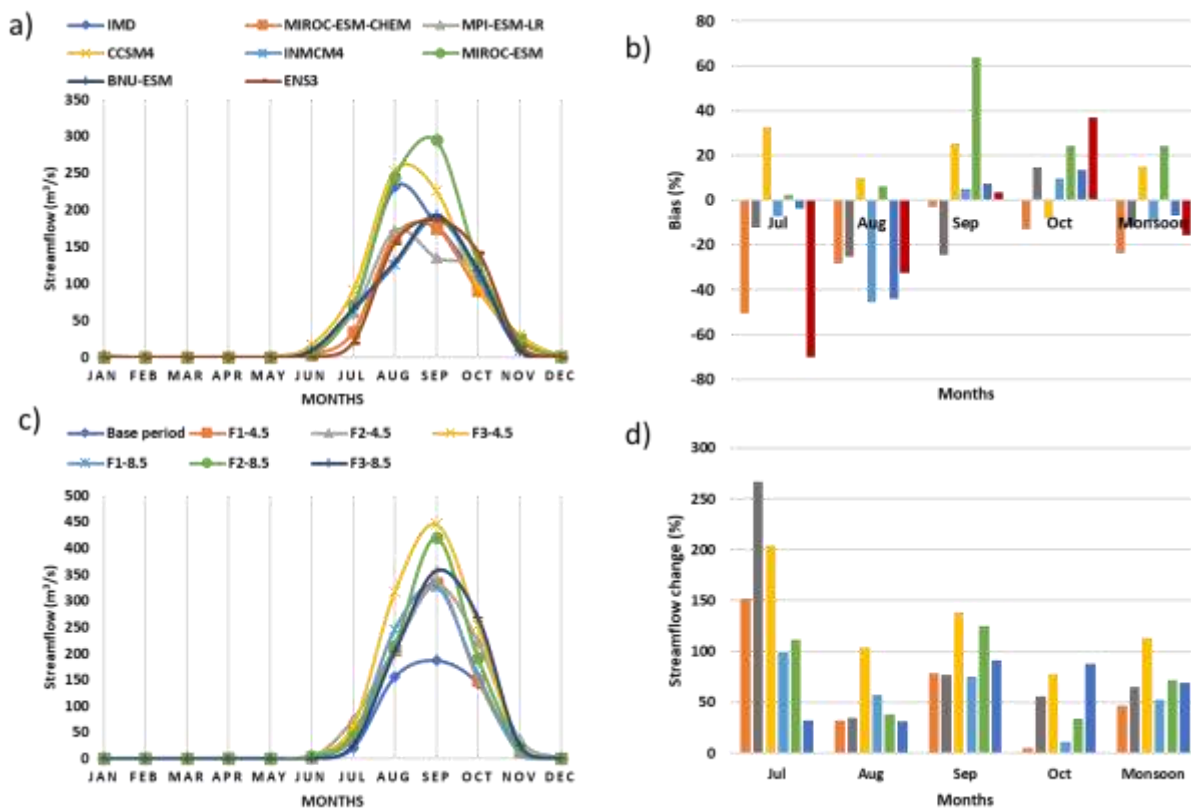
318

319 **Fig. 8** The ensemble model (ENS-3) precipitation and SWAT-simulated streamflow a) during near  
 320 future (2006-2039), b) during mid future (2040-2069) and c) far future (2070-2099) of the Maner  
 321 river basin.

322 **4.4. Mean monthly streamflow in the Maner basin**

323 The average annual monthly streamflows of the CCSM4, MIROC-ESM climate models during the  
 324 base period are shown in Fig 9a, with a bias of 9.83, 6.31, and 25.51, 63.58 in the months of August  
 325 and September, respectively. The remaining four models, MPI-ESM-LR, MIROC-ESM-CHEM,  
 326 BNU-ESM, INMCM4, and ensemble model (ENS3), have low streamflow than other models due  
 327 to less precipitation therefore the corresponding biases of -25.27, -28.46, -43.94, -45.45, and -  
 328 32.56 in the month of August during the base period, respectively (Fig. 9 b). The CCSM4 model  
 329 has an ideal percentage bias and is close to the IMD predicted flow during the base period.  
 330 Similarly, the ensemble model (ENS3) has a reasonable bias percentage of -32.56, 3.63 and +36.85  
 331 % in the months of August, September, and October respectively. As a result, additional analysis  
 332 is performed on the ensemble ENS3 model findings.

333 Because climate models predict high precipitation, the ensemble model future mean monthly  
 334 streamflows are higher than base period flows in August, September, and October (Fig.9 c). Under  
 335 RCP 8.5 and 4.5 scenarios, the mean monthly monsoon streamflow increased in the near, mid, and  
 336 long term. Due to more bias in base period flow, the percentage increase in July is greater, i.e., 250  
 337 percent. Under RCP 4.5 and 8.5 scenarios, the percentage increase in monsoon streamflow is  
 338 46.73, 65.48, 113.528, and 52.77, 71.96, 69.34 in the near, mid, and far future, respectively (Fig.  
 339 9 d). The streamflow percentage increase is more in the month of September i.e., 78.89, 76.55,  
 340 138.74 and 75.3, 125, 91.3 in the near, mid, and far future under RCP 4.5 and RCP 8.5 scenarios,  
 341 respectively because these ensembled models predicted 40 and 33% more precipitation.

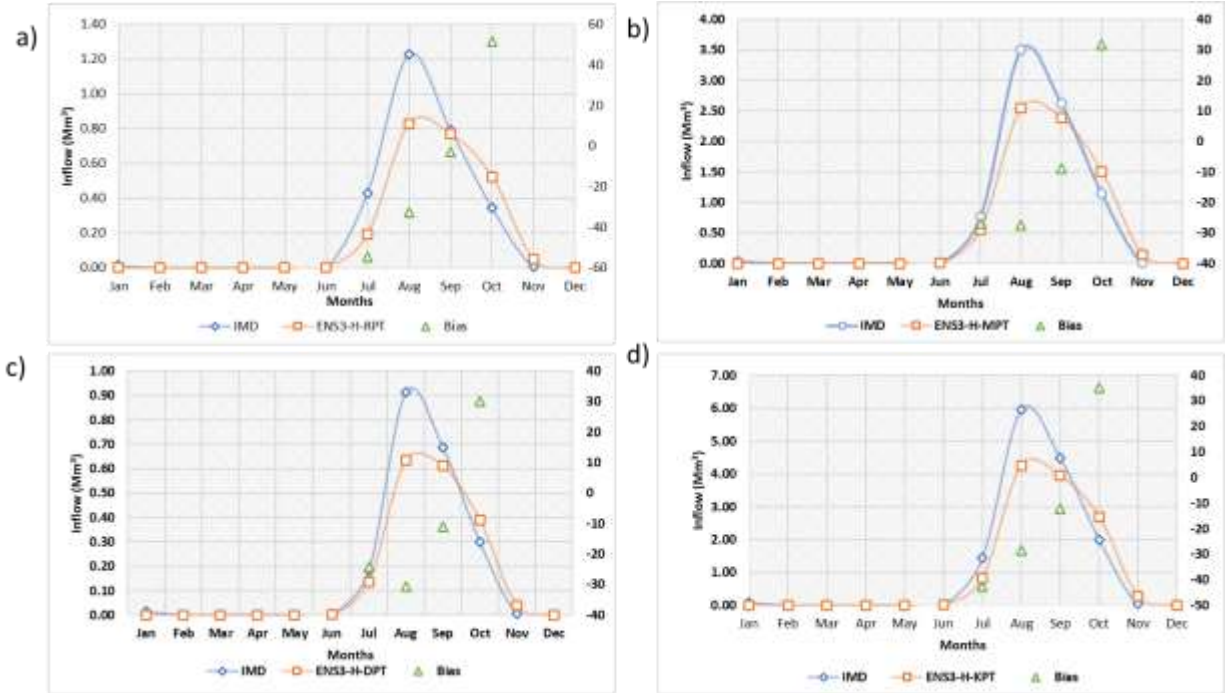


342  
 343 **Fig. 9** a) The mean monthly streamflow of IMD and RCM models, b) the corresponding percentage  
 344 bias during base period (1980-2005), c) the ENS3 future projected streamflow under RCP 4.5 and

345 8.5 scenarios and d) percentage change during near(F1-2006-2039), mid (F2-2040-2069) and far  
346 (F3-2070-2099) future periods in the Maner basin.

#### 347 **4.5. Climate change impact on KTCS**

348 In the cascade arrangement, the inflows to the tanks have increased proportionally with the tank  
349 size. During the base period in August, the IMD and ensemble model simulated tank inflows of  
350 1.2, 3.5, 0.9, 5.94 Mm<sup>3</sup> and 0.83, 2.54, 0.63, 4.26 Mm<sup>3</sup> in Ramchandrapur, Mallampalli,  
351 Dharmaraopalli, Katakshapur tanks (Fig. 10 a-d). The corresponding bias is -32.61, -27.33, -30.58,  
352 -28.54 % in August, -2.7, -8.96, -11.08, -12.2 % in September and 51.38, 31.71, 29.97, 35.02 % in  
353 October months of Ramchandrapur, Mallampalli, Dharmaraopalli, Katakshapur tanks respectively  
354 (Fig.10 a-d). The highest negative and positive biases are observed in August and October months  
355 in Ramchandrapur and Dharmaraopalli tanks as these are small and starting tanks in the cascade.  
356 The average monsoon tank inflows are 2.32, 6.98, 1.77 and 11.74 Mm<sup>3</sup> during base period and  
357 respective biases are -17.1, -12.87, -14.87 and -15.58 in Ramchandrapur, Mallampalli,  
358 Dharmaraopalli and Katakshapur tanks (Fig.10 a-d). These tank monsoon inflow results are similar  
359 to streamflow and the negative bias is due to RCM models being underpredicted and precipitation  
360 shifting during the base period.

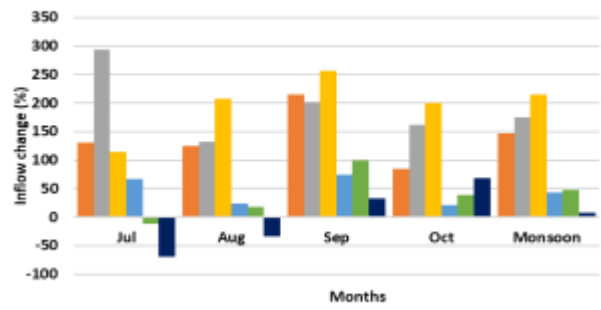
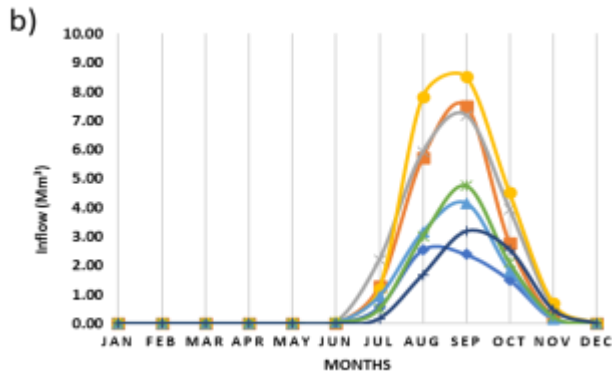
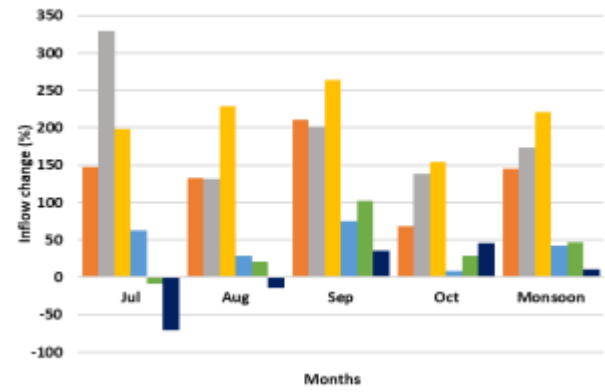
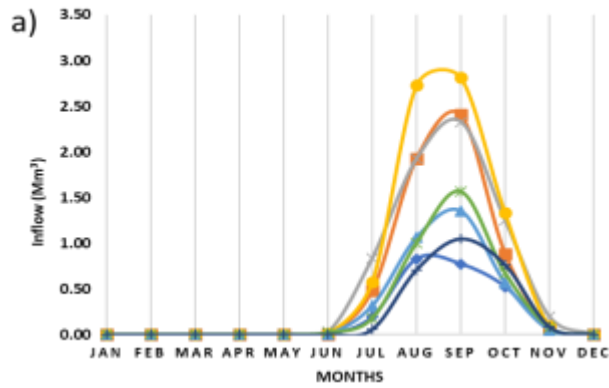


361

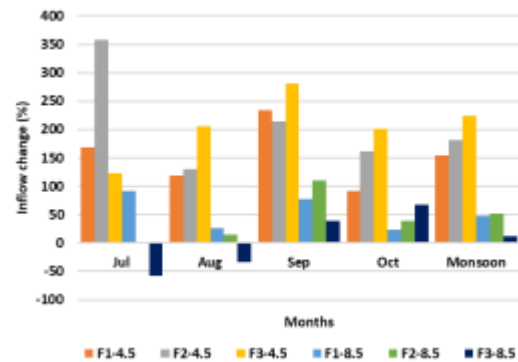
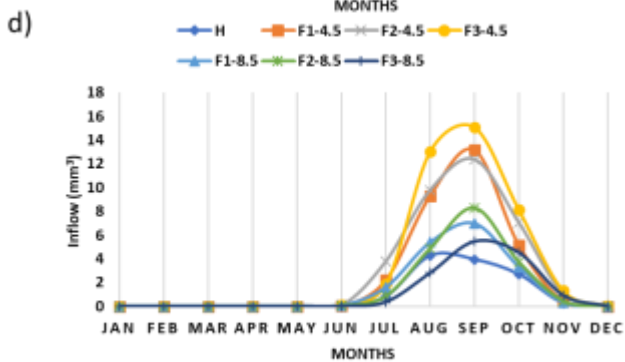
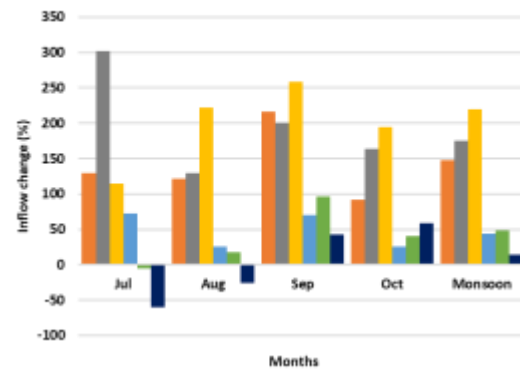
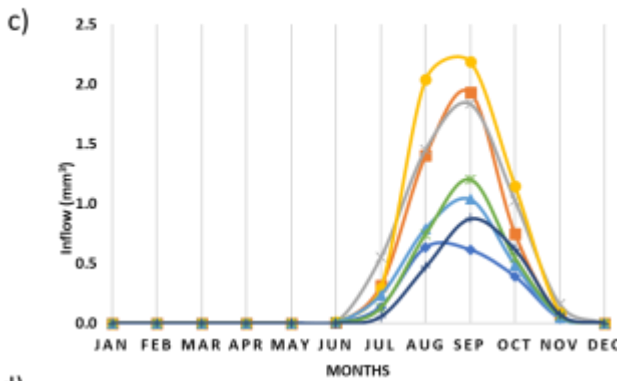
362 **Fig. 10** The IMD and Ensemble (ENS3) model tank inflows and corresponding bias of a)  
 363 Ramchandrapur tank (RPT) b) Mallampalli tank (MPT) c) Dharmaraopalli (DPT) and d)  
 364 Katakshapur (KPT) tanks during base period (1980-2005).

365

366 All tank inflows in KTCS are increased in the near, mid, and far futures compared to the base  
 367 period, but the percentage increase is minimal in the mid-future compared to the near future under  
 368 RCP 4.5 and 8.5 scenarios (Fig 11a-d).



369



370

371 **Fig. 11** The ensemble model mean monthly tank inflows and percentage change of a)  
372 Ramchandrapur b) Mallampalli c) Dharmaraopalli d) Katakshapur tanks for future projected  
373 scenarios during 2022-2099.

374 In comparison to model historical flows, the ensemble model results under RCP 8.5 scenario  
375 projected less inflow than RCP 4.5 scenario in the near, mid, and long term. Under the RCP 4.5  
376 projected scenario, the RPT collects less inflow,  $2.8 \text{ Mm}^3$  (Fig11 a), and the KPT collects more  
377 inflow,  $15 \text{ Mm}^3$  (Fig. 11 d), in the September month among the KTCS tanks. In the future period,  
378 peak inflows will be observed in September, whereas in the base period, they were observed in  
379 August. According to the RCP 4.5 scenario, the inflow of tanks in September will increase by  
380 200% and 250% during the near, mid, and far future periods, respectively (Fig. 11 a-d). The  
381 cascade tanks receive nearly 150, 180 and 220 percentage increase of inflow during the monsoon  
382 (July to October) in near, mid and far future respectively, similar results were noticed in Das and  
383 Umamahesh, 2018 study. In all the tanks of the cascade the maximum increase is nearly 300%  
384 observed in the month of July in mid future under RCP 4.5 scenario, though it is maximum  
385 percentage but the magnitude is less.

#### 386 **4.6. Water balance of the Maner basin and KTCS**

387 Table 4 shows the water balancing components of the Maner river basin. As Precipitation increases  
388 the surface runoff and evapotranspiration is also increased in the future under RCP 4.5 and 8.5  
389 scenarios. Under RCP4.5, the precipitation contribution to surface runoff is 12% in the base period,  
390 14 to 18% and 14 to 17% under RCP8.5 in the near, mid, and far future periods. Evapotranspiration  
391 is the largest contributor to precipitation, accounting for 61.31 % during the base period. Similarly,  
392 61 to 56% and 61 to 60% in near, mid, far future periods under RCP 4.5 and 8.5 respectively, these  
393 results are similar with Nandi et al.,2020. In far future the contribution of surface runoff and  
394 evapotranspiration is increased with respect to base period and near future period in RCP 4.5 and

395 8.5 scenarios. The increase is majorly due to increase in the future precipitation as well increase  
 396 in the urban and agricultural area in the future period.

397 **Table.4** The Average annual Water balance components of the Maner basin

| <b>Period</b>                     | <b>Precipitation<br/>(mm)</b> | <b>Surface Q<br/>(m<sup>3</sup>/s)</b> | <b>ET<br/>(mm)</b> | <b>Total aquifer recharge<br/>(mm)</b> |
|-----------------------------------|-------------------------------|--|--------------------|--|
| ENS3-Base period<br>(H-1980-2005) | 935.6                         | 112.5                                  | 573.6              | 349.57                                 |
| ENS3-RCP4.5-F1                    | 1017.4                        | 149.02                                 | 623.3              | 358.45                                 |
| ENS3-RCP4.5-F2                    | 1084.6                        | 178.39                                 | 640.3              | 387.13                                 |
| ENS3-RCP4.5-F3                    | 1145.6                        | 201.73                                 | 644.9              | 433.8                                  |
| ENS3-RCP8.5-F1                    | 1025.2                        | 150.97                                 | 622.1              | 366.51                                 |
| ENS3-RCP8.5-F2                    | 1092.7                        | 175.45                                 | 647.9              | 392.82                                 |
| ENS3-RCP8.5-F3                    | 1107.4                        | 187.25                                 | 660.8              | 388.97                                 |

398  
 399 The water balancing components of KTCS are shown in Table 5, and the precipitation, surface  
 400 runoff, and evapotranspiration are expected to increase in the future, similar to the Maner basin.  
 401 In the base period, the precipitation contribution to surface runoff and evapotranspiration is 12.51  
 402 and 64.55%, respectively. Surface runoff and evapotranspiration contributions are 15 to 17% and  
 403 59 to 56% in the near, mid, long term under RCP 4.5, and 14 to 16% and 59 to 61 % under RCP  
 404 8.5. Surface runoff contribution increases and evapotranspiration decreases in the far future under  
 405 RCP 4.5 scenario due to decrease in projected precipitation and increase in temperature.

406 **Table.5** The Average annual Water balance components of KTCS

| <b>Period</b> | <b>Precipitation<br/>(mm)</b> | <b>Surface<br/>Q (m<sup>3</sup>/s)</b> | <b>ET (mm)</b> | <b>Total aquifer<br/>recharge (mm)</b> |
|---------------|-------------------------------|--|----------------|--|
|---------------|-------------------------------|--|----------------|--|

|                                   |        |        |       |        |
|-----------------------------------|--------|--------|-------|--------|
| ENS3-Base period<br>(H-1980-2005) | 933.2  | 116.71 | 602.4 | 286.46 |
| ENS3-RCP4.5-F1                    | 1037.5 | 155.92 | 614.2 | 350.89 |
| ENS3-RCP4.5-F2                    | 1097.7 | 183.94 | 631.6 | 370.31 |
| ENS3-RCP4.5-F3                    | 1145.1 | 198.37 | 638.5 | 405.24 |
| ENS3-RCP8.5-F1                    | 1039.2 | 150.34 | 614.2 | 359.46 |
| ENS3-RCP8.5-F2                    | 1092.4 | 172.56 | 642.4 | 365.82 |
| ENS3-RCP8.5-F3                    | 1081.4 | 166.92 | 658.1 | 345.03 |

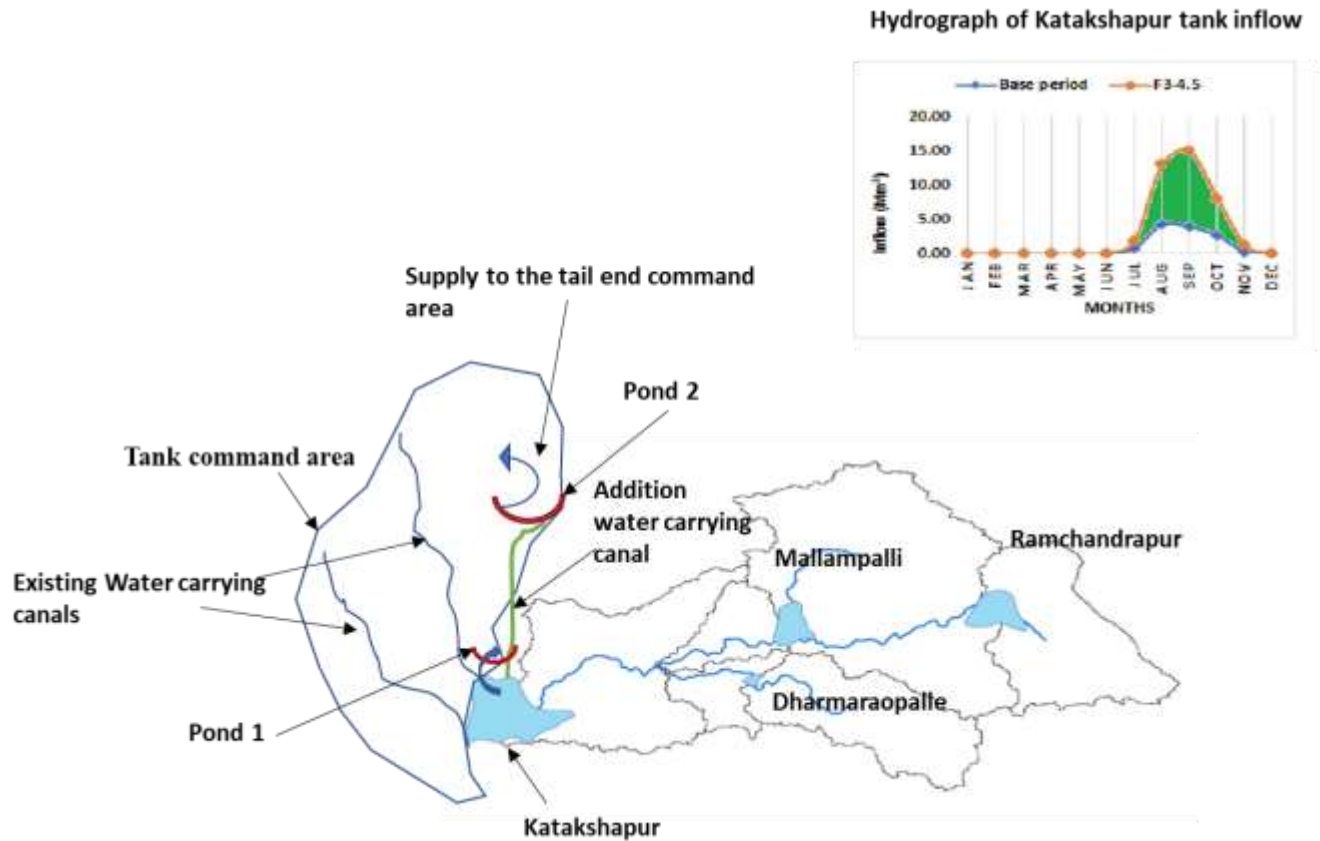
407

408 The main difference between the Maner basin and the KTCS is in total aquifer recharge, which is  
409 349.57 and 286.46 mm during the base period, respectively. Under RCP 4.5 and 8.5 scenarios, the  
410 total aquifer recharge percentage increase in the Maner basin is 2 to 24% and 5 to 11% in the near,  
411 mid, far future. Similarly, the total aquifer recharge percentage increase in KTCS is 22 to 41%,  
412 and 25 to 21% in the near, mid, long term under RCP 4.5 and 8.5 scenarios. Because of the tanks,  
413 the percentage of aquifer recharge is higher in the KTCS than in the Maner basin in all future  
414 periods.

415 **4.7. Sustainable adaptation methods in KTCS**

416 Due to the impact of climate change, the KTCS expect to receive more inflow in far future time  
417 periods compared to base period. Consequently, the Ramchandrapur and Dharmaraopalli tanks are  
418 small and not able to accommodate the excess flow. As result the downstream tank of Katakshapur  
419 receiving more inflow as it is evident from the Hydrograph of Katakshapur given in figure 12.  
420 According to the hydrograph, there will be an additional inflow of 10 Mm<sup>3</sup> of water during month  
421 of September. However, the Katakshapur tank has already receiving significant inflow in previous  
422 months and its maximum capacity is only 18.91 Mm<sup>3</sup>. As a result, the overflow would go to the

423 Salivagu project, which is further downstream and can handle these overflows. If the tank capacity  
424 is increased by removing silt and mud that has settled at the bottom of the tank and by installing  
425 suitable control structures (Sluice gate), the excess flow may be retained in the Katakshapur tank.  
426 To effectively utilize these excess inflows, supply and demand side adaptation methods can be  
427 used. The supply side adaptation is construction of a storage pond-1 and pond 2 at downstream of  
428 the Katakshapur tank overflow section and near the tail end of the command area, where the flow  
429 typically does not reach the end of command area (Fig 12). To maximize the number of farmers  
430 who can benefit, it is essential to both increase the number of borewells in the uplands of the tank  
431 command area and maintain an optimal level of pumping from the wells (Palanisami et al., 2010).  
432 To make use the most of excess tank inflow in the future, several demand-side adaptations are  
433 possible. One option is to provide additional drinking water to the nearby habitats of the near  
434 villages. Another option is to switch to different crops in the command area. Additionally, open  
435 wells can be dug in the fields of the command area to store excess water and use it for percolation  
436 and irrigation during the next crop season. In the far future, these adaptation techniques may be  
437 help to maximize the utilization of surplus inflow received by Katakshapur tank and to increase  
438 the agriculture production.



439

440 **Fig. 12** The schematic diagram of adaptation strategies to sustain the future tank inflow

441 **5. Conclusions**

442 Using the SWAT hydrological model, streamflow and tank inflows were analysed for the Maner  
 443 basin and KTCS under future climate change scenarios of RCP4.5 and 8.5. The ensemble of MPI-  
 444 ESM-LR, MIROC-ESM-CHEM, and CCSM4 models simulated flow is close to base period  
 445 streamflow in all climate model combinations. Among the three models, the CCSM4 is the closer  
 446 to the simulated flow.

447 Under RCP 4.5, the ensemble model monsoon precipitation percentage increase in the near, mid,  
 448 and long term is 13.11, 20.81, and 28.75, respectively, and 14.93, 22.36, and 24.85 under RCP 8.5.

449 Under the RCP4.5 and RCP8.5 scenarios, the maximum monthly precipitation percentage increase

450 is 40 and 51 in September and October of the far future period, respectively. With respect to the  
451 base period, the increase in maximum and minimum temperature is 1.88 °C under RCP 4.5, 3.23  
452 °C and 3.18 °C under RCP 8.5.

453 The simulated flows from IMD closely match the low and medium streamflow magnitudes under  
454 the RCP 8.5 scenario during the historical period from 2006 to 2020 in the ensemble model. The  
455 Maner basin average monsoon (July-October) streamflow percentage increase is 46.73, 65.48, and  
456 113.53 in the near, mid, and long term under RCP 4.5 scenarios, and 52.77, 71.96, and 69.35 under  
457 RCP 8.5 scenarios.

458 Future streamflow peaks in the Maner basin occur in September, with maximum and minimum  
459 peak flows of 1271 m<sup>3</sup>/s and 335.2 m<sup>3</sup>/s in September 2078 and 2045, respectively, under the RCP  
460 4.5 scenario. The upper, middle, and lower Maner dams have the greatest influence on the Maner  
461 river flow and water balance.

462 In KTCS, the inflow into the Ramchandrapur, Mallampalli, Dharmaraopalli, and Katakshapur  
463 tanks increased by 200 percent in the near, mid, and far future periods under the RCP 4.5 scenario.  
464 Similarly, inflows will increase by 150, 180, and 220 percent during the monsoon season (July to  
465 October) in the near, mid, and long term, respectively. The increase is primarily due to the high  
466 precipitation in September.

467 The surface runoff of Maner and KTCS tank inflows increases over time, with the maximum  
468 observed in the far future RCP 4.5 scenario. Katakshapur tank receives the most future inflow  
469 because it is the lowest and largest tank in the KTCS.

470 The contribution of surface runoff and evapotranspiration in the far future is increased in  
471 comparison to the base and near future periods in Maner and KTCS water balances due to increases

472 in precipitation, urban area, and agricultural area. Because of the presence of tank systems, the  
473 percentage of aquifer recharge in KTCS is greater than the overall Maner basin in all future  
474 periods.

475 The storage capacity of the tanks must be increased with appropriate controlling structures to  
476 capture more water and dissipate flooding conditions as adaption strategy. Other adaptation  
477 methods, such as building an artificial recharge pond downstream of the overflow section and in  
478 the fields of command area will improve groundwater recharge. Alternatively, the percolation  
479 ponds can be the strategies outlined in this study can be used to develop policies for sustainable  
480 water management in this region.

481

482 **Declarations**

483 **Ethical Approval** All authors accept all ethical approvals.

484 **Consent to Participate** The authors agree to participate in any survey or feedback task.

485 **Consent to Publish** All authors agree to provide manuscript for publication.

486 **Conflicts of Interest:** The authors declare no conflict of interest.

487 **Author Contributions:**

488 Conceptualization, K.R.; Data curation, R.S. and V.S.; Formal analysis, K.R.; Funding acquisition,  
489 V.R.K.; Project administration, V.R.K.; Resources, V.R.K. and D.P.; Software, R.S.; Supervision,  
490 R.S. and V.S.; Validation, D.P. and V.S.; Writing—original draft, K.R.; Writing—review and  
491 editing, V.S. All authors have read and agreed to the published version of the manuscript.

492 **Funding:** The research described in this paper was carried out with funds provided by the Science  
493 and Engineering Research Board (SERB), DST India through project EMR/2017/004691.

494 **Acknowledgments:** The corresponding author's (V. Sridhar) effort was funded in part by the  
495 Virginia Agricultural Experiment Station (Blacksburg) and through the Hatch Program of the  
496 National Institute of Food and Agriculture at the United States Department of Agriculture  
497 (Washington, DC) and in part as a Fulbright- Nehru senior scholar funded by the United States  
498 India Educational Foundation.

499 **Data Availability Statement:**

500 Datasets will be made available upon request to the authors.

501 **References**

502 Abbaspour, K.C., Vaghefi, S.A., Srinivasan, R., 2017. A guideline for successful calibration and

503 uncertainty analysis for soil and water assessment: A review of papers from the 2016  
504 international SWAT conference. *Water (Switzerland)* 10. <https://doi.org/10.3390/w10010006>

505 Alehu, B.A., Bitana, S.G., 2023. Assessment of Climate Change Impact on Water Balance of Lake  
506 Hawassa Catchment. *Environ. Process.* 10, 14 . <https://doi.org/10.1007/s40710-023-00626-x>

507 Alejo, L.A., Alejandro, A.S., 2022. Changes in Irrigation Planning and Development Parameters  
508 Due to Climate Change. *Water Resour Manage* 36, 1711–1726 .  
509 <https://doi.org/10.1007/s11269-022-03105-4>

510 Allen, R.G., 1986. A Penman for All Seasons. *J. Irrig. Drain. Eng.* 112, 348–368.  
511 [https://doi.org/10.1061/\(asce\)0733-9437\(1986\)112:4\(348\)](https://doi.org/10.1061/(asce)0733-9437(1986)112:4(348))

512 Bekele, E.G., Knapp, H.V., 2010. Watershed Modeling to Assessing Impacts of Potential Climate  
513 Change on Water Supply Availability. *Water Resour. Manag.* 24, 3299–3320.  
514 <https://doi.org/10.1007/s11269-010-9607-y>

515 Bucak, T., Trolle, D., Andersen, H.E., Thodsen, H., Erdoğan, Ş., Levi, E.E., Filiz, N., Jeppesen,  
516 E., Beklioglu, M., Bucak, T., 2017. Future water availability in the largest freshwater  
517 Mediterranean lake is at great risk as evidenced from simulations with the SWAT model. *Sci.*  
518 *Total Environ.* 581–582, 413–425. <https://doi.org/10.1016/j.scitotenv.2016.12.149>

519 Chinnasamy, P., Srivastava, A., 2021. Revival of Traditional Cascade Tanks for Achieving  
520 Climate Resilience in Drylands of South India. *Front. Water* 3, 1–19.  
521 <https://doi.org/10.3389/frwa.2021.639637>

522 Das, J., Umamahesh, N. V., 2018. Spatio-Temporal Variation of Water Availability in a River  
523 Basin under CORDEX Simulated Future Projections. *Water Resour. Manag.* 32, 1399–1419.  
524 <https://doi.org/10.1007/s11269-017-1876-2>

525 Das, J., Umamahesh, N. V., 2016. Downscaling Monsoon Rainfall over River Godavari Basin  
526 under Different Climate-Change Scenarios. *Water Resour. Manag.* 30, 5575–5587.  
527 <https://doi.org/10.1007/s11269-016-1549-6>

528 Dau, Q.V., Kuntiyawichai, K. & Adeloje, A.J., 2021. Future Changes in Water Availability Due  
529 to Climate Change Projections for Huong Basin, Vietnam. *Environ. Process.* 8, 77–98 .  
530 <https://doi.org/10.1007/s40710-020-00475-y>

531 Dessie, M., Verhoest, N. E. C., Pauwels, V. R. N., Adgo, E., Deckers, J., Poesen, J., Nyssen, J.,  
532 2015. Water balance of a lake with floodplain buffering: Lake Tana, Blue Nile Basin,  
533 Ethiopia. *J. Hydrol.* 522, 174–186. <https://doi.org/10.1016/j.jhydrol.2014.12.049>

534 Dibike, Y.B., Coulibaly, P., 2005. Hydrologic impact of climate change in the Saguenay  
535 watershed: Comparison of downscaling methods and hydrologic models. *J. Hydrol.* 307, 145–  
536 163. <https://doi.org/10.1016/j.jhydrol.2004.10.012>

537 Dubey, S.K., Sharma, D., 2018. Assessment of climate change impact on yield of major crops in  
538 the Banas River Basin, India. *Sci. Total Environ.* 635, 10–19.  
539 <https://doi.org/10.1016/j.scitotenv.2018.03.343>

540 Gassman P.W., Reyes, M.R., Green, C.H., Arnold, J.G., 2007 The soil and water assessment tool:  
541 historical development, applications, and future research directions. *Trans ASABE*  
542 50(4):1211–12850.

543 Hassan, D., Burian, S.J., Johnson, R.C. et al., 2022. The Great Salt Lake Water Level is Becoming  
544 Less Resilient to Climate Change. *Water Resour Manage* . [https://doi.org/10.1007/s11269-](https://doi.org/10.1007/s11269-022-03376-x)  
545 [022-03376-x](https://doi.org/10.1007/s11269-022-03376-x)

546 He, S., Guo, S., Yang, G. et al., 2020. Optimizing Operation Rules of Cascade Reservoirs for  
547 Adapting Climate Change. *Water Resour Manage* 34, 101–120.  
548 <https://doi.org/10.1007/s11269-019-02405-6>

549 Hengade, N., Eldho, T.I., 2019. Relative impact of recent climate and land cover changes in the  
550 Godavari river basin, India. *J. Earth Syst. Sci.* 128, 1–17. [https://doi.org/10.1007/s12040-019-](https://doi.org/10.1007/s12040-019-1135-4)  
551 [1135-4](https://doi.org/10.1007/s12040-019-1135-4)

552 Hengade, N., Eldho, T.I., Ghosh, S., 2018. Climate change impact assessment of a river basin  
553 using CMIP5 climate models and the VIC hydrological model. *Hydrol. Sci. J.* 63, 596–614.  
554 <https://doi.org/10.1080/02626667.2018.1441531>

555 Hillard, U., Sridhar, V., Lettenmaier, D.P., McDonald, K.C., 2003. Assessing snow melt dynamics  
556 with NASA Scatterometer (NSCAT) data and a hydrologic process model, *Remote Sensing*  
557 *of Environment*, 86, 52-69, doi: 10.1016/S0034-4257(03)00068-3

558 IITM, 2022: Indian Institute of Tropical Meteorology (IITM), Pune  
559 [http://cccr.tropmet.res.in/home/nex\\_gddp\\_india.jsp](http://cccr.tropmet.res.in/home/nex_gddp_india.jsp), last accessed on 15/2/2022.

560 IMD, 2021, Indian Metrological Department, Pune, [https://www.imdpune.gov.in/Clim\\_Pred\\_LRF\\_](https://www.imdpune.gov.in/Clim_Pred_LRF_New/Grided_Data_Download.html)  
561 [New/Grided\\_Data\\_Download.html](https://www.imdpune.gov.in/Clim_Pred_LRF_New/Grided_Data_Download.html), last accessed on 20/12/2021.

562 IPCC, 2021: Summary for Policymakers. In: *Climate Change 2021: The Physical Science Basis.*  
563 *Contribution of Working Group I to the Sixth Assessment Report of the Intergovernmental*  
564 *Panel on Climate Change* [Masson-Delmotte, V., P. Zhai, A. Pirani, S. L. Connors, C. Péan,  
565 S. Berger, N. Caud, Y. Chen, L. Goldfarb, M. I. Gomis, M. Huang, K. Leitzell, E. Lonnoy,  
566 J.B.R. Matthews, T. K. Maycock, T. Waterfield, O. Yelekçi, R. Yu and B. Zhou (eds.)].  
567 Cambridge University Press.

568 IWRIS, 2022. Indian Water Resources Information System  
569 <https://indiawris.gov.in/wris/#/DataDownload>, last accessed on 20/2/2022

570 Jha, M., Jeffrey, G.A., Phillip, W.G., Flippo, G., Roy, R.G., 2007 Climate change assessment on  
571 Upper Mississippi River Basin streamflows using SWAT. *J Am Water Resour Assoc*

572 42(4):997–1015.

573 Jayanthi, S.L.S.V., Keesara, V.R., 2021. Climate change impact on water resources of medium  
574 irrigation tank. *ISH J. Hydraul. Eng.* 27, 322–333.  
575 <https://doi.org/10.1080/09715010.2019.1649605>

576 Kumar, D.S., 2016. Influence of Climate Variability on Performance of Local Water Bodies:  
577 Analysis of Performance of Tanks in Tamil Nadu, Rural Water Systems for Multiple Uses  
578 and Livelihood Security. Elsevier. <https://doi.org/10.1016/B978-0-12-804132-1.00006-8>

579 Kumar, P., Wiltshire, A., Mathison, C., Asharaf, S., Ahrens, B., Lucas-Picher, P., Christensen,  
580 J.H., Gobiet, A., Saeed, F., Hagemann, S., Jacob, D., 2013. Downscaled climate change  
581 projections with uncertainty assessment over India using a high resolution multi-model  
582 approach. *Sci. Total Environ.* 468–469, S18–S30.  
583 <https://doi.org/10.1016/j.scitotenv.2013.01.051>

584 Leon, A.S., Kanashiro, E.A., Valverde, R., Sridhar, V., 2014. A Dynamic framework for intelligent  
585 control of river flooding- A case study, *ASCE J. Water Resources Planning and Management*,  
586 doi: 10.1061/(ASCE)WR.1943-5452.0000260

587 Madduma Bandara, C.M., 1985. Catchment Ecosystems and Village Tank Cascades in the Dry  
588 Zone of Sri Lanka A Time-Tested System of Land and Water Resource Management 99–113.  
589 [https://doi.org/10.1007/978-94-009-5458-8\\_11](https://doi.org/10.1007/978-94-009-5458-8_11)

590 Melton, F., 2015. NASA Earth Exchange Global Daily Downscaled Projections ( NEX-GDDP ) 1  
591 . Intent of This Document and POC. Guide 1–8.

592 Monteith, J.L., 1965. Evaporation and environment. In *Symposia of the society for experimental*  
593 *biology* (Vol. 19, pp. 205-234). Cambridge University Press (CUP) Cambridge.

594 Maurya, S., Srivastava, P.K., Zhuo, L. et al. 2023. Future Climate Change Impact on the  
595 Streamflow of Mahi River Basin Under Different General Circulation Model Scenarios.  
596 *Water Resour Management*. <https://doi.org/10.1007/s11269-022-03372-1>

597 Nandi, S., Manne, J. Spatiotemporal Analysis of Water Balance Components and Their Projected  
598 Changes in Near-future Under Climate Change Over Sina Basin, India. *Water Resour Manage*  
599 34, 2657–2675 (2020). <https://doi.org/10.1007/s11269-020-02551-2>

600 Neitsch, S.L., Arnold, J.G., Kiniry, J.R., Williams, J.R., 2001. Soil and water assessment tool  
601 theoretical documentation version 2000. Grassland, Soil and Water Research Service,  
602 Temple.

603 Neitsch, S.L., 2005. Soil and water assessment tool. User's Manual Version 2005, 476.

604 Pai D.S., Latha Sridhar, Rajeevan M., Sreejith O.P., Satbhai N.S. and Mukhopadhyay B.,  
605 2014: Development of a new high spatial resolution (0.25° X 0.25°) Long period (1901-2010)

606 daily gridded rainfall data set over India and its comparison with existing data sets over the  
607 region; MAUSAM, 65, 1(January 2014), pp1-18.Pant, G. B. and Rupa Kumar, K., *Climates*  
608 *of South Asia*, John Wiley & Sons, Chichester, 1997, pp. 320

609 Saraf, V.R., Regulwar, D.G., 2018. Impact of Climate Change on Runoff Generation in the Upper  
610 Godavari River Basin, India. *J. Hazardous, Toxic, Radioact. Waste* 22, 04018021.  
611 [https://doi.org/10.1061/\(asce\)hz.2153-5515.0000416](https://doi.org/10.1061/(asce)hz.2153-5515.0000416)

612 Satish Kumar, K., Rathnam, E., Sridhar, V., 2020. Tracking seasonal fluctuations of drought  
613 indices with GRACE terrestrial water storage over major river basins in South India, *Science*  
614 *of the Total Environment*, doi: 10.1016/j.scitotenv.2020.142994.

615 Sharmila, S., Joseph, S., Sahai, A.K., Abhilash, S., Chattopadhyay, R., 2015. Future projection of  
616 Indian summer monsoon variability under climate change scenario: An assessment from  
617 CMIP5 climate models. *Glob. Planet. Change* 124, 62–78.  
618 <https://doi.org/10.1016/j.gloplacha.2014.11.004>

619 Sharannya, T.M., Mudbhatkal, A. & Mahesha, A., 2018. Assessing climate change impacts on  
620 river hydrology – A case study in the Western Ghats of India. *J Earth Syst Sci* 127, 78.  
621 <https://doi.org/10.1007/s12040-018-0979-3>

622 Sowjanya. P, N., Venkata Reddy, K., Shashi, M., 2020. Intra- and interannual streamflow  
623 variations of Wardha watershed under changing climate. *ISH J. Hydraul. Eng.* 26, 197–208.  
624 <https://doi.org/10.1080/09715010.2018.1473057>

625 Sridhar, V., Billah, M.M., Hildreth, J., 2018. Coupled Surface and Groundwater Hydrological  
626 Modeling in a Changing Climate, *Groundwater*, 56, 4, 618-635, doi:10.1111/gwat.12610

627 Srinivasan, R., Ramanarayanan, T.S., Arnold, J.G., Bednarz, S.T., 1998. LARGE AREA  
628 HYDROLOGIC MODELING AND ASSESSMENT PART II: MODEL APPLICATION. *J.*  
629 *Am. Water Resour. Assoc.* 34, 91–101. <https://doi.org/10.1111/j.1752-1688.1998.tb05962.x>

630 Srivastava, A., Chinnasamy, P., 2021. Water management using traditional tank cascade systems:  
631 a case study of semi-arid region of Southern India. *SN Appl. Sci.* 3, 1–23.  
632 <https://doi.org/10.1007/s42452-021-04232-0>

633 A. K. Srivastava, Rajeevan, M., Kshirsagar, S.R., 2009. Development of High Resolution Daily  
634 Gridded Temperature Data Set (1969-2005) for the Indian Region. *ATMOSPHERIC*  
635 *SCIENCE LETTERS Atmos. Sci. Let.* DOI: 10.1002/asl.232.

636 Thiery, W., Davin, E.L., Panitz, H.J., Demuzere, M., Lhermitte, S., Van Lipzig, N., 2015. The  
637 impact of the African Great Lakes on the regional climate. *J. Clim.* 28, 4061–4085.  
638 <https://doi.org/10.1175/JCLI-D-14-00565.1>

639 Uniyal, B., Jha, M.K., Verma, A.K., 2015. Assessing Climate Change Impact on Water Balance  
640 Components of a River Basin Using SWAT Model. *Water Resour. Manag.* 29, 4767–4785.

641 <https://doi.org/10.1007/s11269-015-1089-5>

642 Van Meter, K.J., Steiff, M., McLaughlin, D.L., Basu, N.B., 2016. The socioecohydrology of  
643 rainwater harvesting in India: Understanding water storage and release dynamics across  
644 spatial scales. *Hydrol. Earth Syst. Sci.* 20, 2629–2647. [https://doi.org/10.5194/hess-20-2629-](https://doi.org/10.5194/hess-20-2629-2016)  
645 2016

646 Veijalainen, N., Dubrovin, T., Marttunen, M., Vehviläinen, B., 2010. Climate Change Impacts on  
647 Water Resources and Lake Regulation in the Vuoksi Watershed in Finland. *Water Resour.*  
648 *Manag.* 24, 3437–3459. <https://doi.org/10.1007/s11269-010-9614-z>

649 Vema, V., Sudheer, K.P., Rohith, A.N. et al. 2022. Impact of water conservation structures on the  
650 agricultural productivity in the context of climate change. *Water Resour Manage* 36, 1627–  
651 1644 (2022). <https://doi.org/10.1007/s11269-022-03094-4>

652 Venkata Rao, G., Keesara, V.R., Sridhar, V., Srinivasan, R., Umamahesh, N.V., Pratap, D., 2020.  
653 Spatio-Temporal Analysis of Rainfall Extremes in the Flood-prone Nagavali and Vamsadhara  
654 Basins in Eastern India, *Weather and Climate Extremes*, 29, 100265, doi:  
655 10.1016/j.wace.2020.100265.

656 Von Oppen, M., Subba Rao, K., 1987. Tank Irrigation in Semi-Arid Tropical India: Economic  
657 Evaluation and Alternatives for Improvement. *Agric. Econ.*

658 Zhang, Y., Jun, X., Tao, L., Quanxi, S., 2009. Impact of water projects on river flow regimes and  
659 water quality in Huai River basin. *Water Resour Manag.* doi:10.1007/s11269-009-9477-3

660